Bohdan Andriyevsky
Chair of Foundations of Electronics
Faculty of Electronics and Computer Sciences
Koszalin University of Technology, Poland

Vasyl' Kurlyak
Mykola Romanyuk
Volodymyr Stakhura
Chair of Experimental Physics
Faculty of Physics
I. Franko National University of L'viv, Ukraine

Vasyl' Stadnyk
Chair of Solid State Physics
Faculty of Physics
I. Franko National University of L'viv, Ukraine

Electronic-and-optical properties of Rb_2ZnCl_4 crystals

1. Introduction

The crystals of dirubidium tetrachlorozincate, Rb_2ZnCl_4, are a typical example of the incommensuratelly modulated structures A_2BX_4. They experience the standard for these crystals sequence of phase transitions (PT): paraelectric phase (T_i = 302 K) → incommensurate phase (T_C = 192 K) → commensurate phase [1 - 3]. The high temperature phase I of the crystal is paraelectric with the space group of symmetry *Pnam* (no. 62) and the corresponding unit cell contains four formula units, $Z = 4$. The intermediate phase II ($T_C < T < T_i$) is incommensurately modulated in the *a*-direction of unit cell with the wave vector $\boldsymbol{q} = (1 - \delta)\boldsymbol{a}^*/3$. The low temperature phase III ($Pna2_1$, $\boldsymbol{q} = \boldsymbol{a}^*/3$) is improper ferroelectric one with the spontaneous polarization vector along *c*-axis and triple unit cell dimension along *a*-axis. At the temperature 74 K, the crystal undergoes phase transition into the monoclinic structure of $C1c1$ space group of symmetry, which in fact is doubled related to the structure of $Pna2_1$ along *b*-axis and contains 48 formula units [3, 4].

The incommensurate phase of Rb_2ZnCl_4 has been studied by the method of electron diffraction. Below T_i, additional blurred spots appear on the diffraction

pattern, which are responsible for appearance the incommensurate phase in the crystal with additional modulation in *a*-direction [5, 6].

Previously, temperature dependencies of the birefringence $\delta(\Delta n_i)$ of Rb_2ZnCl_4 for only one wavelength have indicated that deviation from the linear dependency $\delta(\Delta n_i) = k \cdot T$ in the paraelectric phase are observed at decreasing temperature long before T_i [7 - 9]. The linear electro-optic effect is not observed in the incommensurate phase of the crystal because macroscopically this phase remains center symmetrical [9, 10].

In spite of the considerable interest, complex study of the refractive properties of Rb_2ZnCl_4 in wide spectral and temperature ranges is not jet done. The probable influence of the uniaxial mechanical stresses on the refractive properties and he temperatures T_C and T_i of the crystal are also not studied. Previously, considerable uniaxial baric sensitivity of the refractive index and birefringence had been indicated for the isomorphic K_2ZnCl_4 crystal [11, 12]. We do not know any theoretical *ab initio* reference study on the electronic band structure and optical properties of Rb_2ZnCl_4.

In the present study, theoretical results of first principles calculations of electronic and optical properties and experimental results of refractive properties of the mechanically free and uniaxially stresses Rb_2ZnCl_4 crystal are presented.

2. Methods of investigations

Calculations of the electronic structure and optical properties of Rb_2ZnCl_4 have been performed by the CASTEP program [13], based on the density functional theory (DFT) and plane-waves, with using the ultrasoft pseudopotentials [14]. The generalized gradient approximation (GGA) for the exchange and correlation effects [15] and the cutoff energy 340 eV for the plane-waves basis set were used. The electronic eigen-energy convergence tolerance was chosen to be $2.4 \cdot 10^{-7}$ eV and the tolerance for the electronic total energy convergence during crystal structure optimization was $1 \cdot 10^{-5}$ eV. Also, the corresponding maximum ionic force tolerance was $3 \cdot 10^{-2}$ eV/Å and the maximum stress component tolerance was taken to be $5 \cdot 10^{-2}$ GPa. Optimization (relaxation) of the atomic positions and crystal's unit cell parameters at every value of the external stress was performed before the calculations of the electronic characteristic: total electronic energy *E*, band energy dispersion $E(K)$, partial density of electronic states (PDOS), and dielectric functions $\varepsilon(\hbar\omega)$. Band structure of the crystal was calculated for 34 *K*-points of the Brillouin zone (BZ) at the space group of symmetry no. 62. The calculations were performed using the semi-empirical dispersion interaction correction module taking into account the van-der-Waals interactions between atoms [16].

Single crystals Rb_2ZnCl_4 were grown from water solutions using the method of slow cooling. The grown crystals had a form of the rhombic prisms with a lot of facets. Experimental measurements of refractive indices n_i and its changes under uniaxial mechanical stress σ_m were performed using the method described in [17]. Analysis of baric changes of the principal refractive indices n_i of the crystal was performed using the following definition of the piezo-and-optical coefficient π_{im} [18],

$$\delta a_i = \pi_{im}\sigma_m, \quad i,m = 1,2,...,6, \tag{1}$$

where

$$\delta a_i = \delta\left(\frac{1}{n_i^3}\right) = -\frac{2\delta n_i}{n_i^3}. \tag{2}$$

3. Results and discussion

The refractive index dispersion $n_i(\lambda)$ of Rb_2ZnCl_4 crystal have been measured in the wavelength range λ 270 nm to 750 nm for different light polarizations ($i = x, y, z$) and uniaxial stresses at ambient temperature (Fig. 1). In this spectral range, the dispersion of mechanically free and stressed samples is normal ($dn_i/d\lambda < 0$) and its absolute value increases rapidly when the wavelength reaches the long wavelength edge of fundamental absorption of the crystal. It is also seen from figure 1 that the uniaxial stresses do not change the character of the curves $n_i(\lambda)$, but change only the dispersion magnitude $dn_i/d\lambda$ ($dn_a/d\lambda = 12{,}7\cdot10^{-5}$ and $12{,}0\cdot10^{-5}$, $dn_b/d\lambda = 11{,}2\cdot10^{-5}$ and $10{,}6\cdot10^{-5}$, and $dn_c/d\lambda = 12{,}1\cdot10^{-5}$ and $11{,}8\cdot10^{-5}$ in the wavelength region near $\lambda = 500$ nm for the mechanically free and uniaxially stressed samples by the pressure $\sigma_z = 200$ bar, respectively).

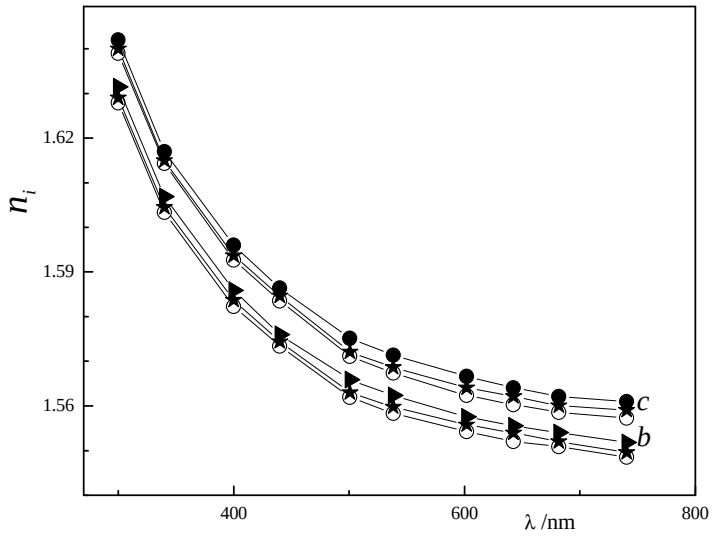

Figure 1. Refractive index dispersion curves of Rb_2ZnCL_4 crystal at ambient temperature and external compression 200 bar (0.02 GPa) ($i = b$, c – crystallographic axes, o - mechanically free sample, ● - compression along b-axis, ▶ - compression along c-axis, ∑ - compression along a-axis)

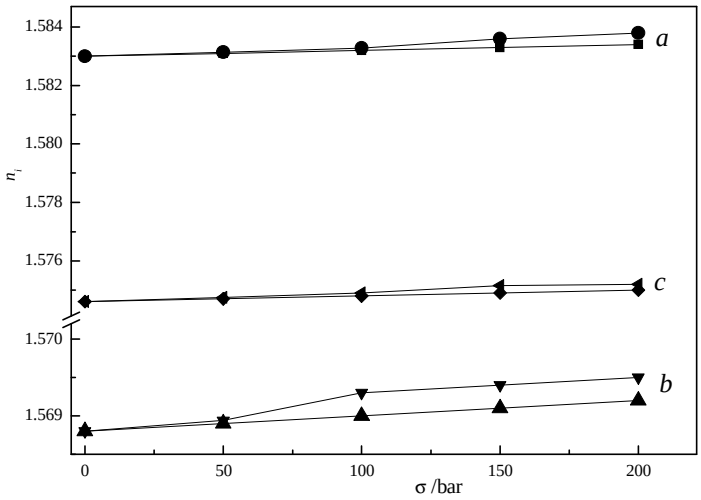

Figure 2. Baric dependencies of principal refractive indices n_i ($\lambda = 500$ nm) of Rb_2ZnCL_4 crystal at ambient temperature ($i = a$, b, c – crystallographic axes, ● - compression along c-axis, ■ - compression along b-axis, ▼ - compression along a-axis)

The averaged specific increase of refractive indices caused by the uniaxial compression is found to be near $dn_i/d\sigma \approx 2 \cdot 10^{-6}$ bar^{-1} (Fig. 2).

Band structures and dielectric functions $\varepsilon(\hbar\omega)$ of Rb_2ZnCl_4 have been calculated for the space groups no. 62. The total energy E_t of the crystal is equal to -18685.755 eV (without dispersion corrections) and -18691.574 eV (with dispersion corrections). So, the difference $\Delta E_t = 5.82$ eV may be regarded as a characteristic parameter of the van-der-Waals interaction in Rb_2ZnCl_4.

The calculated energy band gap of the crystal is found to be $E_g = 4.47$ eV (Γ - Γ), that is expected to be approximately 1 eV to 2 eV smaller than corresponding experimental value, because of the known features of the local density approximation of DFT [19]. This band gap E_g corresponds to the Γ - Γ transition of the Brillouin zone.

Analysis of Rb_2ZnCl_4 partial density of states have revealed that highest valence bands of the crystal are formed mainly by the *p*-states of oxygen and lowest conduction bands originate from the *s*-states of rubidium and zinc. Energy positions of the valence bands partial density of states maxima of Rb_2ZnCl_4 are found to be very similar to those for K_2ZnCl_4 crystals obtained by using the *ab initio* VASP code [20]. The only differences concern to the PDOS of potassium in K_2ZnCl_4 and rubidium in Rb_2ZnCl_4. Results of our calculation are in moderate agreement with the photoelectron spectra of Rb_2ZnCl_4 [21].

We have calculated also the elastic coefficients of Rb_2ZnCl_4 (space group no. 62) on the basis of the relaxed structure of the crystal (Table 1), which may be compared with the experimental data [22]. These data may be useful for the analysis of piezo-optical properties of the crystal.

Table 1. Elastic modulus *B* and coefficients of elastic stiffness c_{ij} (*i*, *j* = 1, 2, ... 6) of Rb_2ZnCl_4 calculated at space groups no. 62 (*a* = 9.33 Å, *b* = 12.6 Å, *c* = 7.10 Å, *V* = 835 Å^3). All values are in GPa units.

	B	c_{11}	c_{22}	c_{33}	c_{12}	c_{13}	c_{23}	c_{44}	c_{55}	c_{66}
no. 62	15	38	22	33	8	11	8	7	11	7

Optical functions of crystals originated from the electronic excitations are calculated in CASTEP on the basis of the wave functions Ψ and band structure energies *E*. The imaginary part of the dielectric function $\varepsilon_2(\hbar\omega)$ is obtained from the following relation [23],

$$\varepsilon_2(\hbar\omega) = \frac{2e^2\pi}{V\varepsilon_0} \sum_{\boldsymbol{K},v,c} \left| \langle \Psi_{\boldsymbol{K}}^c \left| \hat{\boldsymbol{u}} \cdot \boldsymbol{r} \right| \Psi_{\boldsymbol{K}}^v \rangle \right|^2 \delta\left(E_{\boldsymbol{K}}^c - E_{\boldsymbol{K}}^v - \hbar\omega \right) \quad (3)$$

and then the corresponding real part $\varepsilon_1(\hbar\omega)$ is calculated using the following Kramers-Kronig equation.

$$\varepsilon_1(\hbar\omega)-1=\frac{2}{\pi}\int_0^{\infty}\frac{t\varepsilon_2(t)dt}{t^2-(\hbar\omega)^2} \tag{4}$$

The indices of absorption (k) and refraction (n) are connected with the real (ε_1) and imaginary (ε_2) parts of the complex dielectric function of a material according to the know relations: $\varepsilon_1 = n^2 - k^2$, $\varepsilon_2 = 2nk$.

The calculated optical properties of Rb_2ZnCl_4 are presented in figure 3. The calculated spectra of absorption index $k(\hbar\omega)$ of Rb_2ZnCl_4 (Fig. 3) are in moderate agreement with the experimental reflectance spectra of the crystal obtained in the photon energy range 0 eV to 35 eV with using the synchrotron radiation [21]. Position of the main maximum of the calculated spectrum $k(\hbar\omega)$ at $\hbar\omega = 10$ eV agrees well with magnitude of the corresponding experimental maximum of the reflection spectrum $R(\hbar\omega)$. Large difference of our calculated spectrum $k(\hbar\omega)$ and experimental one $R(\hbar\omega)$ in the range $\hbar\omega < 8$ eV is explained by the excitonic effects occurred in this spectral range, which are not taken into account in the DFT-based calculations of optical properties using CASTEP code. Also, the calculated energy band gap E_g of the crystal ($E_g \approx 4.5$ eV) is much smaller than the corresponding value $E_g \approx 8.0$ eV estimated in the reference [21] on the basis of analysis of the excitonic structure of Rb_2ZnCl_4 with two maxima located in the energy range 7.0 eV to 8.0 eV. Besides, the underestimated value of the calculated band gap E_g of Rb_2ZnCl_4 was expected because of the known features of the DFT local density approximation.

Experimental and calculated refractive indices of Rb_2ZnCl_4 are presented in Table 2.

Table 2. Refractive indices n_x. n_y. and n_z of Rb_2ZnCl_4: experimental (at photon energy $\hbar\omega = 1.68$ eV) and calculated (at photon energy $\hbar\omega = 0.01$ eV) for mechanically free ($\sigma = 0$) and uniaxially stressed crystal ($\sigma_x = \sigma_y = \sigma_z = 1$ GPa).

	Experimental	Theoretical			
		$\sigma = 0$	σ_x	σ_y	σ_z
n_x	1.5660	1.6429	1.6401	1.6530	1.6483
n_y	1.5525	1.6240	1.6215	1.6330	1.6295
n_z	1.5564	1.6292	1.6264	1.6444	1.6297

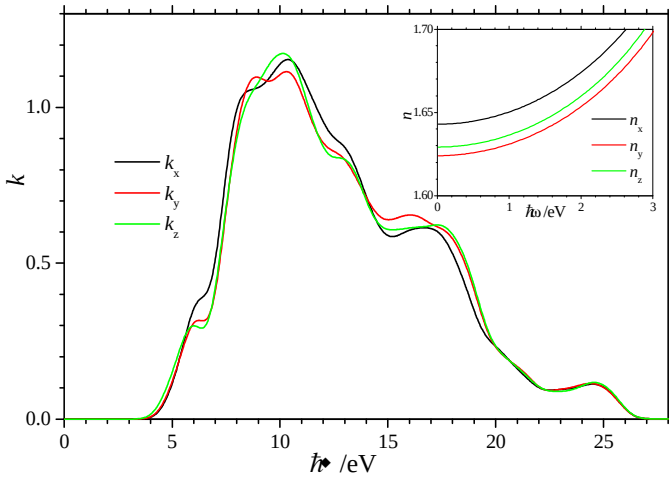

Figure 3. Calculated spectral dependencies of absorption $k_i(\hbar\omega)$ and refractive $n_i(\hbar\omega)$ indices of Rb_2ZnCl_4 (refractive index dispersions are presented in inset).

Higher theoretical values of the refractive indices in relation to the corresponding experimental ones (Table 2) are caused by the known features of the local density approximation used in DFT [19].

We have calculated several piezo-optical coefficients π_{im} for Rb_2ZnCl_4 using the data in Table 2. The components of the piezo-optical tensor π_{im}, corresponding to only uniaxial stresses (k = 1, 2, 3) are presented in Table 3. Positive sign of π_{im} correspond to the decrease of refractive index under compression of a crystal.

Table 3. Components of the tensor of stress elastic-and-optical coefficients π_{im} based on refractive indices of Rb_2ZnCl_4 at photon energy $\hbar\omega$ = 0.01 eV (in units 10^{-12} Pa^{-1}).

π_{im}	m = 1	m = 2	m = 3
i = 1	1,29	-4,54	-2,43
i = 2	1,19	-4,19	-2,54
i = 3	1,31	-7,00	-0.22

Anisotropy of the coefficients π_{im} in relation to the uniaxial stress direction m observed in Table 3 is inversely proportional to the corresponding anisotropy of the elastic stiffness constants c_{ii} (Table 1). This is caused by the inverse dependency of the refractive index n and the unit cell volume V (see relations 3 and 4).

Therefore, the piezo-optical coefficient based on the value $\chi V = (n^2 - 1)V$ (the value χV is proportional to the unit cell electronic polarizability α [24]) should reflect sensitivity of electronic polarizability to the external stress more properly than that (π_{im}) based on the value of refractive index n. The value χV was already

used for the study of influence of the uniaxial stresses on the optical properties of K_2SO_4 crystals [20].

Table 4. Components of the tensor $\chi_{ii}V$ (i = 1, 2, 3) (at photon energy $\hbar\omega$ = 0.01 eV) for relaxed (σ = 0) and mechanically stressed (σ_{ii} = 1 GPa) Rb_2ZnCl_4 crystal ($\chi_{av}V$ is an averaged component) and corresponding band gap E_g. The relative changes are indicated in brackets.

$\chi_{ii}V$ Stress	$\chi_{11}V$ Å^3	$\chi_{22}V$ Å^3	$\chi_{33}V$ Å^3	$\chi_{av}V$ Å^3	E_g eV
σ = 0	1419	1367	1381	1389	4.467
σ_{11}	1403 (-0.011)	1352 (-0.011)	1365 (-0.012)	1373 (-0.011)	4.542 (0.017)
σ_{22}	1412 (-0.005)	1358 (-0.007)	1388 (0.005)	1386 (-0.002)	4.550 (0.019)
σ_{33}	1416 (-0.002)	1365 (-0.001)	1366 (-0.011)	1382 (-0.005)	4.296 (-0.038)

The relative changes $\delta(\chi_{ii}V)/\chi_{ii}V$ of the value $\chi_{ii}V$ under an influence of the uniaxial compression of 1 GPa on Rb_2ZnCl_4 do not exceed the range -1.2% to 0.5% (Table 4), that means rather small corresponding changes of the electronic polarizability of the crystal. The relative averaged changes $\delta(\chi_{av}V)/\chi_{av}V$ was found to be negative for all three principal directions of the uniaxial compression (Table 4). It is remarkable that absolute values $|\delta(\chi_{av}V)/\chi_{av}V|_{ii}$ correlate with corresponding refractive indices n_{ii} and unit cell electronic polarizabilities $\chi_{ii}V$ of the relaxed Rb_2ZnCl_4 crystal. On the other hand side, baric changes of the energy band gap E_g look uncorrelated with the corresponding changes of refractive indices (n) and unit cell polarizability (χV).

4. Conclusions

Partial density of states of Rb_2ZnCl_4 are found to be very similar to those obtained earlier for K_2ZnCl_4 crystals, that indicates for similarity of the electronic structure in two crystals, which in turn is due to the common anion $ZnCl_4^{2-}$.

Changes of the energy band gap E_g of Rb_2ZnCl_4 under the uniaxial compression along the principal crystallographic axes i (i = 1, 2, 3) were found to be uncorrelated with the corresponding changes of the refractive indices n_{ii} and the unit cell electronic polarizability $\chi_{ii}V$ of the crystal.

The relative changes of the unit cell electronic polarizability of Rb_2ZnCl_4 under an influence of the uniaxial compression of 1 GPa do not exceed the values -1.2% to

0.5%, that indicates small baric changes of the corresponding electronic polarizability.

Anisotropy of the piezo-optical coefficients π_{ii} of Rb_2ZnCl_4 in relation to the uniaxial stress direction is found to be inversely proportional to the corresponding anisotropy of the elastic stiffness constants c_{ii}.

References

1. S. R. Andrews, H. J. Mashiyama. *J. Phys. C.: Sol. State Phys.* **16** (1983) 4985.
2. M. Quilichini, J. Panetier. *Acta Cryst. B* **39** (1983) 657.
3. Sh. Hirotsu, K. Toyota, K. Hamano. *J. Phys. Soc. Jap.* **46** (1979) 1389.
4. H. M. Lu and J. R. Hardy. *Phys. Rev. B* **45** (1992) 7609.
5. R. Blinc, B. Losar, F. Milia, R. Kind. *J. Phys C.: Solid State Phys.* **17** (1984) 241.
6. K. Tsuda, N. Yamamoto, K. Yagi. *J. Phys. Soc. Jap.* **57** (1988) 2057.
7. S.V. Melnikova, A.T. Anistratov. *Phys. Solid State* **25** (1983) 848 (in Russian).
8. P. Gunter, R. Sunctuary, F. Rohner, H. Arend, N. Seidenbusch. *Solid State Commun.* **37** (1981) 883.
9. J. Kroupa, J. Fousek. *Jap. J. of Appl. Phys.* **24** (1985) 787.
10. R. Sunctuary, P. Gunter. *Phys. Stat. Solidi (a)* **84** (1984) 103.
11. V.Yo. Stadnyk, M. O. Romanyuk , B. V. Andrievsky, Z. O. Kohut. *Optics and Spectroscopy* **108** (2010) 753.
12. M. Gaba, V. Yo. Stadnyk, Z. O. Kohut, R. S. Brezvin. *J. Appl. Spectr.* **77** (2010) 648.
13. S. J. Clark, M. D. Segall, C. J. Pickard, P. J. Hasnip, M. J. Probert, K. Refson, M. C. Payne, *Zeitschrift fuer Kristallographie* **220** (2005) 567.
14. D. Vanderbilt, *Phys. Rev. B* **41** (1990) 7892.
15. J.P. Perdew, K. Burke, M. Ernzerhof, *Phys. Rev. Lett.* **77** (1996) 3865.
16. E.R. McNellis, J. Meyer, K. Reuter, *Phys. Rev. B* **80** (2009) 205414.
17. V.Yo. Stadnyk, M.O. Romanyuk, R.S. Brezvin. *Electronic polarizability of ferroics*. L'viv: I. Franko LNU Publ. (2013). 392 pp. (in Ukrainian)
18. T. S. Narasimhamurty *Photoelastic and Electro-Optic Properties of Crystals*. – New York and London.: Plenum Press 1981. 514 pp.
19. J. P. Perdew, *Int. J. Quantum Chem.* **28** (1985) 497.
20. B. Andriyevsky, V. Stadnyk, Z. Kohut, M. Romanyuk, M. Jaskólski, *Mater. Chem. Phys.* **124** (2010) 845.
21. A. Ohnishi, M. Saito, M. Kitaura, M. Itoh, M. Sasaki, *J. Lumin.* **132** (2012) 2639.

22. A.V. Kityk, . V.P. Soprunyuk, O.G. Vlokh, *Phys. Status Solidi (a)* **138** (1993) 119.
23. http://www.tcm.phy.cam.ac.uk/castep/documentation/WebHelp/CASTEP.html.
24. M. Born, E. Wolf, *Principles of Optics*, Pergamon, Oxford, 1984.

Abstract

Electronic-and-optical properties of Rb_2ZnCl_4 crystal have been studied using the theoretical and experimental methods. First principles calculations of the electronic structure and optical properties using the density functional theory have been performed on the relaxed and uniaxially compressed (1 GPa) Rb_2ZnCl_4 crystal. The refractive indices of Rb_2ZnCl_4 have been measured in the spectral range of wavelength 300 nm to 750 nm for three principal uniaxial compression stresses (0.02 GPa) at room temperature. *Ab initio* calculations and analysis have revealed that the observed uniaxial pressure changes of the refractive indices of Rb_2ZnCl_4 are caused mainly by the corresponding changes of the crystal unit cell dimensions. The unit cell electronic polarizability of the crystal remains approximately unchanged.

Streszczenie

Zbadano właściwości elektronowo-optyczne kryształów Rb_2ZnCl_4 metodami teoretyczną i doświadczalną. Wykonano obliczenia z pierwszych zasad (*ab initio*) struktury elektronowej i właściwości optycznych na bazie teorii funkcjonału gęstości zrelaksowanych i jednoosiowo ściśniętych (1 GPa) kryształów. Zostały pomierzone współczynniki załamania Rb_2ZnCl_4 w przedziale długości fal światła 300 nm do 750 nm dla trzech głównych krystalograficznych kierunków ściskania (0.02 GPa) przy temperaturze pokojowej. Obliczenia *ab initio* i analiza danych ujawniły, że obserwowane baryczne zmiany współczynników załamania Rb_2ZnCl_4 są spowodowane głównie odpowiednimi zmianami rozmiarów komórki elementarnej kryształu. Przy tym, polaryzowalność elektronowa komórki kryształu pozostaję się prawie niezmienną.